Mechanisms Underlying the Formation and Dynamics of Subcellular Calcium Alternans in the Intact Rat Heart

Gary L. Aistrup, Yohannes Shiferaw, Sunil Kapur, Alan H. Kadish and J. Andrew Wasserstrom

Circ. Res. 2009;104;639-649; originally published online Jan 15, 2009;
DOI: 10.1161/CIRCRESAHA.108.181909
Circulation Research is published by the American Heart Association. 7272 Greenville Avenue, Dallas, TX 72514
 Print ISSN: 0009-7330. Online ISSN: 1524-4571

Mechanisms Underlying the Formation and Dynamics of Subcellular Calcium Alternans in the Intact Rat Heart

Gary L. Aistrup,* Yohannes Shiferaw,* Sunil Kapur, Alan H. Kadish, J. Andrew Wasserstrom

Abstract—Optical mapping of intact cardiac tissue reveals that, in some cases, intracellular calcium (Ca) release can alternate from one beat to the next in a large-small-large sequence, also referred to as Ca transient (CaT) alternans. CaT alternans can also become spatially phase-mismatched within a single cell, when one part of the cell alternates in a large-small-large sequence, whereas a different part alternates in a small-large-small sequence, a phenomenon known as subcellular discordant alternans. The mechanisms for the formation and spatiotemporal evolution of these phase-mismatched patterns are not known. We used confocal Ca imaging to measure CaT alternans at the sarcomeric level within individual myocytes in the intact rat heart. After a sudden change in cycle length (CL), 2 distinct spatial patterns of CaT alternans emerge. CaTs can form spatially phase-mismatched alternans patterns after the first few beats following the change in CL. The phase mismatch persists for many beats, after which it gradually becomes phase matched via the movement of nodes, which are junctures between phase-mismatched cell regions. In other examples, phase-matched alternans gradually become phase-mismatched, via the formation and movement of nodes. In these examples, we observed large beat-to-beat variations in the cell activation times, despite constant CL pacing. Using computer simulations, we explored the underlying mechanisms for these dynamical phenomena. Our results show how heterogeneity at the sarcomeric level, in conjunction with the dynamics of Ca cycling and membrane voltage, can lead to complex spatiotemporal phenomena within myocytes of the intact heart. **(*Circ Res*. 2009;104:639-649.)**

Key Words: alternans ■ subcellular calcium cycling ■ confocal microscopy ■ computer modeling ■ intact heart

Calcium release within a cardiac myocyte occurs within thousands of spatially distributed microdomains where membrane-bound L-type Ca channel (LCC) openings trigger the activation of ryanodine receptor (RyR) channels.[1] During a normal beat, the action potential (AP) ensures that Ca release is synchronized throughout the cell, whereas electrotonic coupling between cells ensures that Ca release is synchronized between neighboring cells. However, optical Ca-imaging techniques have revealed that intracellular Ca can, under certain conditions, exhibit rich spatiotemporal properties within single myocytes[2,3] and in cardiac tissue.[4,5] Aistrup et al[3] used high-resolution confocal microscopy to image intracellular Ca release in whole heart and found that Ca transients (CaTs) could vary substantially within different parts of the cell and also between neighboring cells during rapid pacing. It is not yet understood why, and under what conditions, these asynchronous release patterns emerge.

During rapid pacing, CaTs can alternate in a large-small-large-small (L-S-L-S) sequence from one beat to the next.[6–8] CaT alternans are thought to originate from a period-doubling instability,[9,10] which can occur because of the dependence of the AP duration (APD) on the previous diastolic interval or via a steep Ca release versus sarcoplasmic reticulum (SR) load relationship, ie, a nonlinearity that originates because of Ca-cycling dynamics.[11,12] Confocal microscopic studies[2,3,13] have shown that CaT alternans in a region of a cell can alternate in a L-S-L-S sequence, whereas a neighboring region can alternate in a S-L-S-L sequence, a phenomenon known as subcellular discordant alternans. These patterns can be complex because several regions of the cell can alternate with different temporal sequences.[2,3] In this article, we refer to this phenomenon as phase-mismatched CaT alternans, as opposed to phase-matched CaT alternans where all regions of the cell alternate with the same temporal sequence. The presence of phase-mismatched CaT alternans is potentially arrhythmogenic because large intracellular Ca gradients are formed between phase-mismatched regions. The presence of these large gradients may then induce Ca waves[14] to propagate between cellular regions, which could induce triggered activity such as delayed afterdepolarizations.[15,16] Furthermore, subcellular heterogeneity attributable to phase-mismatched alternans may induce voltage heterogeneities on the tissue scale. This can happen, for instance, if the density and distribution of phase-mismatched regions vary substan-

Original received June 19, 2008; revision received January 4, 2009; accepted January 7, 2009.

From the Departments of Molecular Pharmacology and Biological Chemistry (G.L.A.) and Medicine (S.K., A.H.K., J.A.W.) and the Feinberg Cardiovascular Research Institute (S.K., A.H.K., J.A.W.), Feinberg School of Medicine, Northwestern University, Chicago, Ill; and Department of Physics (Y.S.), California State University, Northridge.

*Both authors contributed equally to this work.

Correspondence to Gary L. Aistrup, PhD, S215, 303 E Chicago Ave, Chicago, IL 60611. E-mail glais@northwestern.edu

Circulation Research **is available at http://circres.ahajournals.org** **DOI: 10.1161/CIRCRESAHA.108.181909**

tially between different cardiac regions. Because subcellular Ca influences membrane voltage via Ca-sensitive currents such as the sodium/calcium exchanger (NCX) and the LCC current, spatial heterogeneity of Ca can induce heterogeneities in membrane voltage. These heterogeneities of voltage may then contribute to impulse propagation abnormalities.[17]

Little is known about the properties of phase-mismatched alternans in cardiac cells. Numeric simulation studies have investigated the mechanisms underlying these patterns and have shown that they have rich dynamical properties that are governed by the bidirectional coupling between intracellular Ca release and membrane voltage.[18,19] However, much of this work has not been experimentally validated and the underlying mechanisms are not established. In this study, we applied a combined experimental and mathematical modeling approach to investigate the spatiotemporal dynamics of subcellular Ca cycling during rapid pacing. We hypothesized that phase-mismatched CaT patterns arise because of heterogeneities in Ca-cycling properties at the sarcomeric level. To test this hypothesis, we measured Ca release at the single sarcomere level within cardiac myocytes in the intact heart. Our findings show that dynamical factors such as CaT and cycle length (CL) alternans can amplify spatial heterogeneities in the cell to yield phase-mismatched CaT alternans. Moreover, the patterns of subcellular CaTs are dynamic and evolve in a manner that is dictated by the bidirectional coupling between membrane voltage and Ca.

Materials and Methods

Real-Time Confocal Ca Fluorescence (CaT) Acquisition

The whole rat heart preparation and recording of CaTs at sarcomeric-level resolution in ventricular myocytes of intact epicardium have been described in detail elsewhere.[3] Additional details are provided in the expanded Materials and Methods section in the online data supplement, available at http://circres.ahajournals.org.

Mathematical Model

To model the subcellular spatial organization of CaT alternans, we divided the cell into 100 sarcomeres, and each sarcomere was modeled using a set of ordinary differential equations describing Ca cycling within that sarcomere. The essential elements of the local Ca-cycling machinery are based on the model of Shiferaw et al[12] and are given in detail in the online data supplement.

Results

Subcellular CaT Alternans Development After an Abrupt Change to Rapid Pacing

Line scan recordings of CaTs obtained in individual myocytes (36 cells from 11 hearts) during episodic pacing demonstrated that CaT alternans formed after an abrupt increase in rate. In all cases, if CaT alternans formed, they were phase-matched across the whole cell for the first 2 beats after the change in CL. For intermediate CLs (typically 160 to 140 ms at 35°C, 300 to 260 ms at 24°C), subcellular alternans remained phase matched throughout the rapid pacing epoch, whereas at faster pacing (typically CLs=140 to 100 ms at 35°C, 260 to 180 ms at 24°C), the CaT alternans evolved toward a phase-mismatched pattern in the subsequent ≈3 to 10 beats. Once formed, phase-mismatched CaT alternans persisted for varying duration of rapid pacing, which depended on both temperature and pacing CL. The X-t line scan in Figure 1A illustrates this subcellular CaT alternans development–persistence–cessation process in a myocyte consisting of 67 "sarcomeres" (2-μm partitions) after an abrupt change in pacing CL from 500 ms to 120 ms. Sarcomeric CaTs are periodic and exhibit no alternans during baseline pacing but, during the first 3 cycles of rapid pacing, sarcomeric CaTs immediately exhibit varying degrees of alternans with a matched L-S spatiotemporal phase. Within several cycles, however, the spatiotemporal phases of the alternans of various sarcomeric CaTs become mismatched. This is illustrated in the selected sarcomeric CaT fluorescence versus time profiles shown in Figure 1B. During cycles 1 to 4, sarcomeric CaT nos. 66 and 2 exhibit alternans of L-S-L-S, whereas sarcomeric CaT no. 22 exhibits L-S-L-L. Thus, after cycle 3 (t_0), the alternans of sarcomeric CaT no. 22 is out of phase with those of nos. 2 and 66. Within the limits of our resolution, the alternans of sarcomeric CaT nos. 6 to 55 are phase-matched after cycle 3 but phase-mismatched with those of sarcomeric CaT nos. 1 to 5 and nos. 56 to 67. At least 2 nodes,[20,21] junctures of mismatched phases, develop after cycle 3 (at t_0). However, as is depicted by the dashed white lines overlaying the X-t line scan image in Figure 1A, the nodes are not stationary and travel to the cell ends and disappear, at t_1 for the "lower" node and at t_2 for the "upper" node. Phase reversal of the alternans of sarcomeric CaT nos. 1 to 5 and nos. 56 to 67 occurs when the respective nodes pass through them. Note that in the example average fluorescence versus time profiles of sarcomeric CaT nos. 2 and 66, little if any alternans are exhibited at the moment (2 cycles) each node passes through. After t_2, the alternans of all sarcomeric CaTs are phase-matched again.

By plotting poststimulus latencies of CaT initiation, peak and duration at 90% recovery (TD_{90}) versus each "sarcomere," and aligning the plot with the corresponding X-t line scan image (Figure 1C), it is clear that there is significant spatiotemporal heterogeneity in sarcomere SR Ca release and reuptake along the length of the myocyte during baseline pacing in this example (and in all cells examined). However, heterogeneity in latency of Ca release does not predict the specific location of node development and movement, indicating that static heterogeneities alone are insufficient to explain the dynamic movement of phase-mismatched Ca alternans. Some nominal predictive power seemed to be offered by plotting sarcomeric CaT integrals (Figure 1D) (ie, high, narrow distributions of CaT integral measures seem to coincide with the initial location of node development) perhaps because this parameter encompasses both amplitude and time.

Late Development of Phase-Mismatched CaT Alternans During Rapid Pacing

In some myocytes, sarcomeric CaT alternans that are phase-matched across the whole cell after many beats can gradually become phase-mismatched. This behavior is distinct from that observed in Figure 1A, where CaT alternans were phase-mismatched shortly after the change in CL but then became phase-matched for the remainder of pacing. This behavior is shown in Figure 2A, where we observe the same

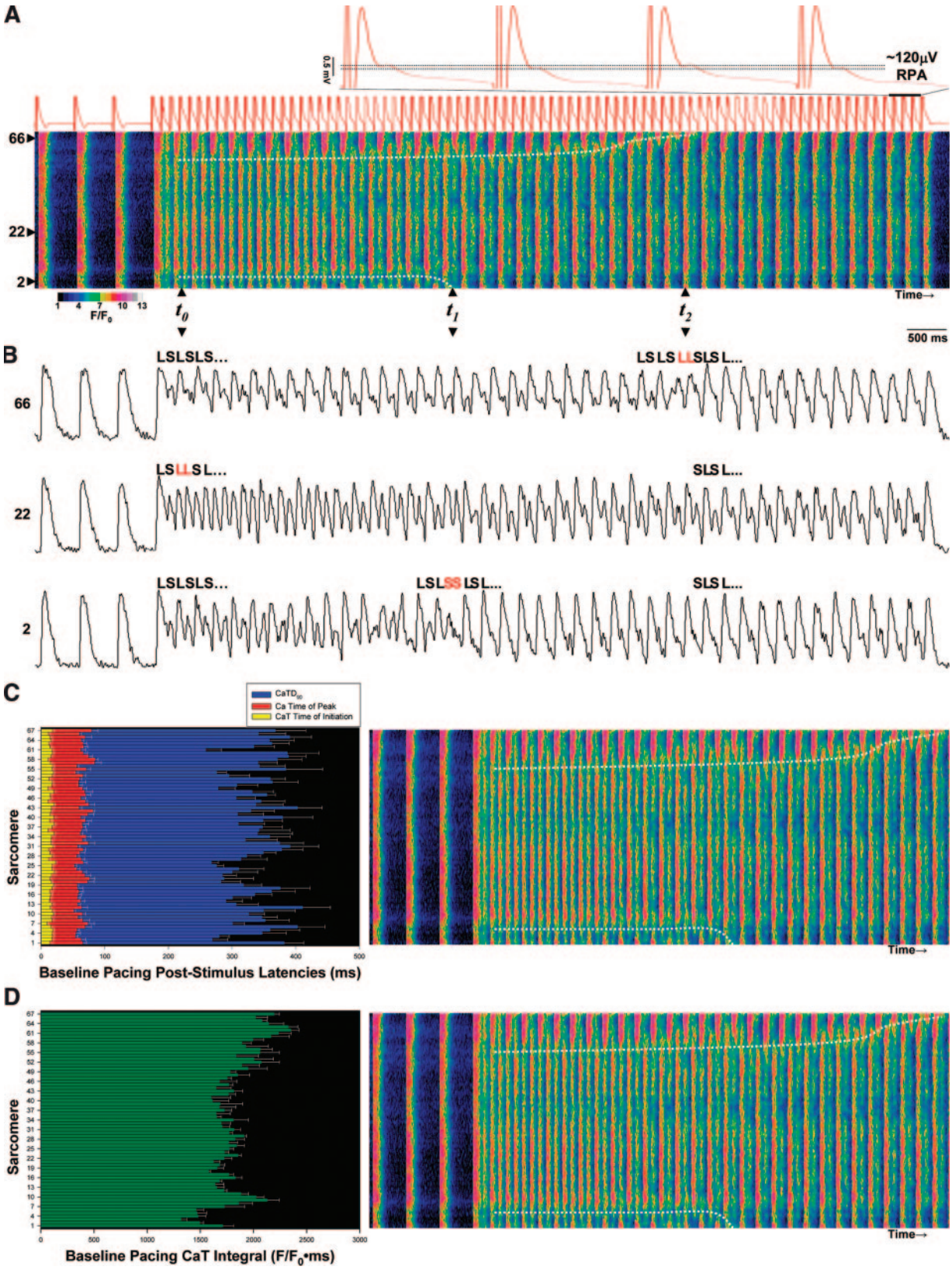

Figure 1. Spatiotemporal evolution and dynamics of subcellular CaT alternans after abrupt change to rapid pacing. A, Confocal CaT fluorescence line scan image of a myocyte in the ventricular epicardium during baseline pacing (CL=500 ms) and during rapid pacing (CL=120 ms). Red tracing above the image is the corresponding pECG. The last 4 beats of the pECG are expanded above. B, Average fluorescence (F) vs time (t) profiles of selected sarcomeric CaTs during pacing. C, Comparison of mean times±SEM from stimulus to initiation, peak, and TD_{90} for all sarcomeres during baseline pacing with corresponding line scan image to the right. D, Comparison of mean amplitude·time integrals±SEM of Ca release and reuptake for each sarcomere during baseline pacing with corresponding line scan image to the right.

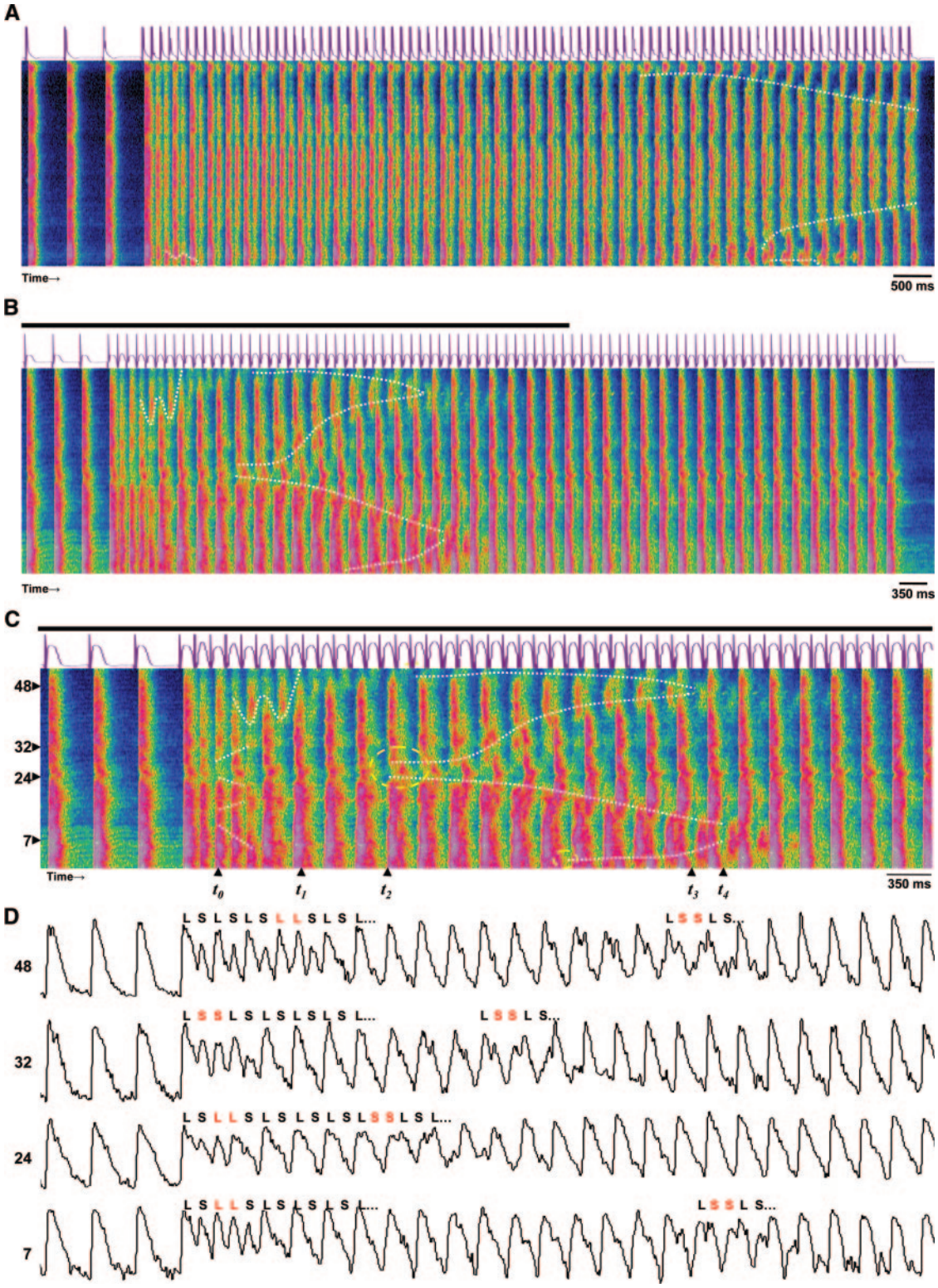

Figure 2. Spatiotemporal evolution and dynamics of subcellular CaT alternans during constant rapid pacing. A, Line scan image of a myocyte during baseline pacing and then during the rapid test train at CL=115 ms. B, Image from another myocyte from another heart during baseline pacing at CL=350 ms and then during the rapid test train at CL=120 ms. C, Time expansion of the period in the line scan image in B (denoted by bold black horizontal line above image) showing the development and cessation of the initial session of alternans (t_0 to t_1) and later redevelopment (yellow dashed circles) and cessation of multinodal subcellular CaT alternans (t_2 to t_4). D, Average fluorescence (F) vs time profiles of select sarcomeric CaTs extracted from B.

mapping field as that shown in Figure 1, with baseline pacing CL=500 ms and rapid pacing CL=115 ms. The myocyte in this example is adjacent to that shown in Figure 1, illustrating that distinct spatiotemporal phenomena can emerge in response to small changes in CL. Alternans are phase-matched for the first 55 beats, and on the 55th beat, 2 nodes emerge from the top and bottom of the cell and drift toward the center of the cell (Figure 2A). A multinodal example of this behavior is shown in Figure 2B. The line scan in Figure 2C is a time-expanded version of Figure 2B, from which select sarcomeric average fluorescence versus time profiles are displayed in Figure 2D. As in Figure 1, the initial period of multinodal subcellular CaT alternans begins immediately after changing to rapid pacing, and extinguishes over t_0 to t_1 as the alternans of all sarcomeric CaTs eventually become spatiotemporally phase-matched when the nodes travel and collide with each other or with the ends of the cell, followed by 5 cycles of phase-matched CaT alternans. Starting at time t_2, however, sarcomeric CaTs in 3 different regions (dashed yellow circles) again begin to exhibit phase-mismatched alternans. In this case 2 "inner" nodes form spontaneously inside the cell and travel toward opposite ends of the cell, whereas 2 "outer" nodes traveled toward the center of the cell. Again, the phase of the sarcomeric CaT alternans reverses as the nodes pass through their respective regions, and eventually inner and outer nodes meet at times t_3 and t_4, after which all sarcomeric CaT alternans are once again phase-matched.

A close inspection of these and other examples of more complex CaT alternans dynamics revealed that the timing of Ca activation varied significantly from beat-to-beat. However, because we have not measured the local membrane voltage, we can only infer the time of activation from the sarcomere CaTs. Our rationale is that when an electrical wavefront passes through the cell in the mapping field, the local membrane voltage will rise rapidly on a time scale <1 ms. This rapid rise of the membrane voltage induces the opening of LCCs distributed throughout the cell. Activation of LCCs is a fast process and occurs on a time scale of roughly 1 to 5 ms and triggers Ca release throughout the cell via Ca-induced Ca release (CICR).[1] Because CICR is also a fast process (5 to 10 ms), we can estimate the time of cell activation by simply identifying that time when subcellular regions of uniform Ca release occur. Uniform Ca release across the >20-μm subcellular regions typically observed during image acquisition cannot be explained by simple diffusion of Ca, because it is too slow to correlate activation times across such intracellular spans. Using the examples of Figure 2A and 2B, we have illustrated our estimations of cell activation in Figure 3A and 3B. Note that we verify these measurements of cell activation of very small whole-cell or subcellular CaTs by measuring the initiation of Ca release in adjacent cells that gave sufficiently large CaTs during these same cycles, an interaction between neighboring myocytes that may also have some bearing on the formation of discordant CaT alternans at the cellular and/or regional level.[22] Our analysis of rapid pacing epochs indicated that whereas the CLs of the electrical stimuli delivered were precisely those set, the local CLs for actual Ca release in the recording site often developed beat-to-beat short–long alternations (or CL alternans) that grew with time, often becoming >10 ms.

Simulation Results

Evolution of Phase-Mismatched Alternans: Constant CL

Our experimental results revealed a variety of distinct spatiotemporal properties associated with both CaT and CL alternans. Here, we will apply mathematical modeling to simulate these properties and elucidate their underlying mechanisms. As a starting point, we examine Figure 1 and note that sarcomeric CaTs exhibit heterogeneities in their beat-to-beat characteristics after the change in CL. Based on this observation, we hypothesized that the initial alternans phase for a given sarcomere depends on the Ca-cycling characteristics of that sarcomere. Thus, the phase mismatch that developed over the next few beats should be a direct consequence of differences in Ca-cycling properties across sarcomeres, which could be attributable to a variety of factors such as spatial variations in expression levels of NCX, SERCA2a (sarco-/endoplasmic reticulum Ca-ATPase), or LCC.

To test the role of heterogeneity in the formation of phase-mismatched Ca alternans, we modeled a cell as a collection of coupled sarcomeres and endowed each sarcomere with different Ca-cycling characteristics. Heterogeneity can arise because of any number of factors that influence Ca cycling, such as variations in protein expression. In these studies, we modeled variations in SR Ca release properties, because this is the variable which has the most direct effect on Ca cycling and should vary to some degree between sarcomeres. To modulate Ca release, we allow each sarcomere to have specific Ca release properties by simply controlling the slope (u) of the SR Ca release versus SR Ca load relationship,[12] which in our simplified model includes the combined effect of RyR channel density, dyadic junction spacing, and RyR Ca sensitivity on both the cytosolic and luminal sides. Heterogeneity in Ca cycling was incorporated into a simulated myocyte such that sarcomeres 1 to 20 and sarcomeres 80 to 100 have a slope $u=12$ sec^{-1}, whereas sarcomeres 21 to 79 have slope $u=14$ sec^{-1} (Figure 4A). We then simulated the dynamical response of this heterogeneous distribution of sarcomeres after a jump from baseline pacing (CL=400 ms) to rapid pacing (CL=200 ms). Plotting the intracellular Ca concentrations ($[Ca]_i$) versus time across the whole cell shows that phase-mismatched alternans form after the first few beats following the change in CL. Two nodes form at the junctures between subcellular regions of lower and higher u, and each node travels toward opposing cell ends. In Figure 4B, we plot the $[Ca]_i$ versus time profiles for selected individual sarcomeres 15, 50, and 90. The first 6 cycles after the rate increase show that sarcomeres 15 and 90 both exhibit the CaT alternans sequence L-S-L-S-L, whereas sarcomere 50 displays an alternans sequence L-S-S-L-S-L. Thus the spatiotemporal phase of the alternans in sarcomere 50 is mismatched with those of sarcomeres 15 and 90 after only 2 short cycles. This phase-mismatched pattern persists for 30 short cycles, indicating that Ca diffusion between sarcomeres was insufficient to disperse the phase-mismatch. However, the phase-mismatched pattern was dynamic and the nodes

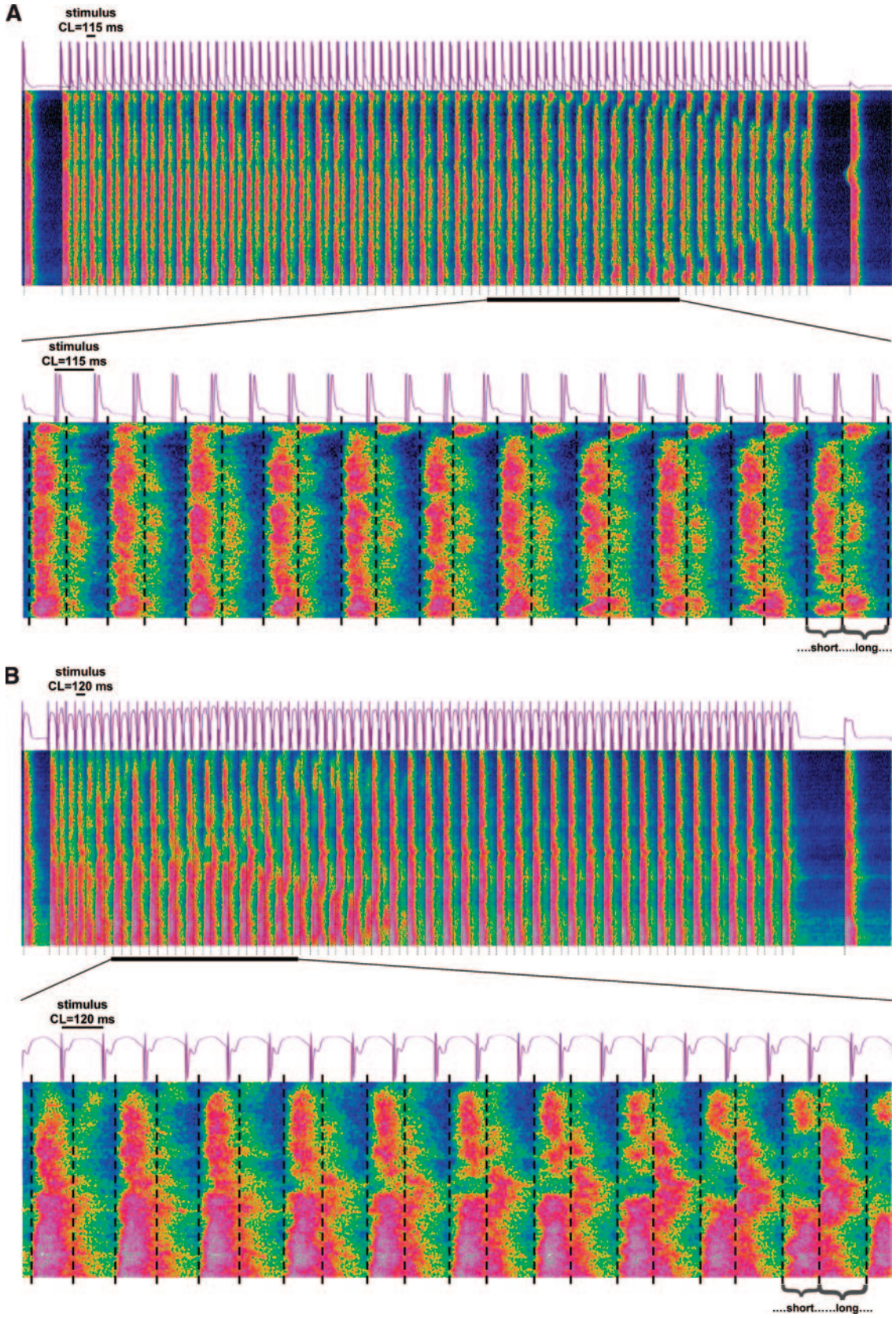

Figure 3. CL alternans during rapid pacing. A, Top, Same line scan image as in Figure 2A showing one baseline pacing cycle, the rapid pacing epoch, and an intrinsic beat following pacing (with pECG above the image). Dashed black vertical lines denote timing of cell activations as determined by uniform Ca release. Bottom, Time expansion of image in A (denoted by bold black horizontal line). B, Descriptions as in A for the line scan image in Figure 2B.

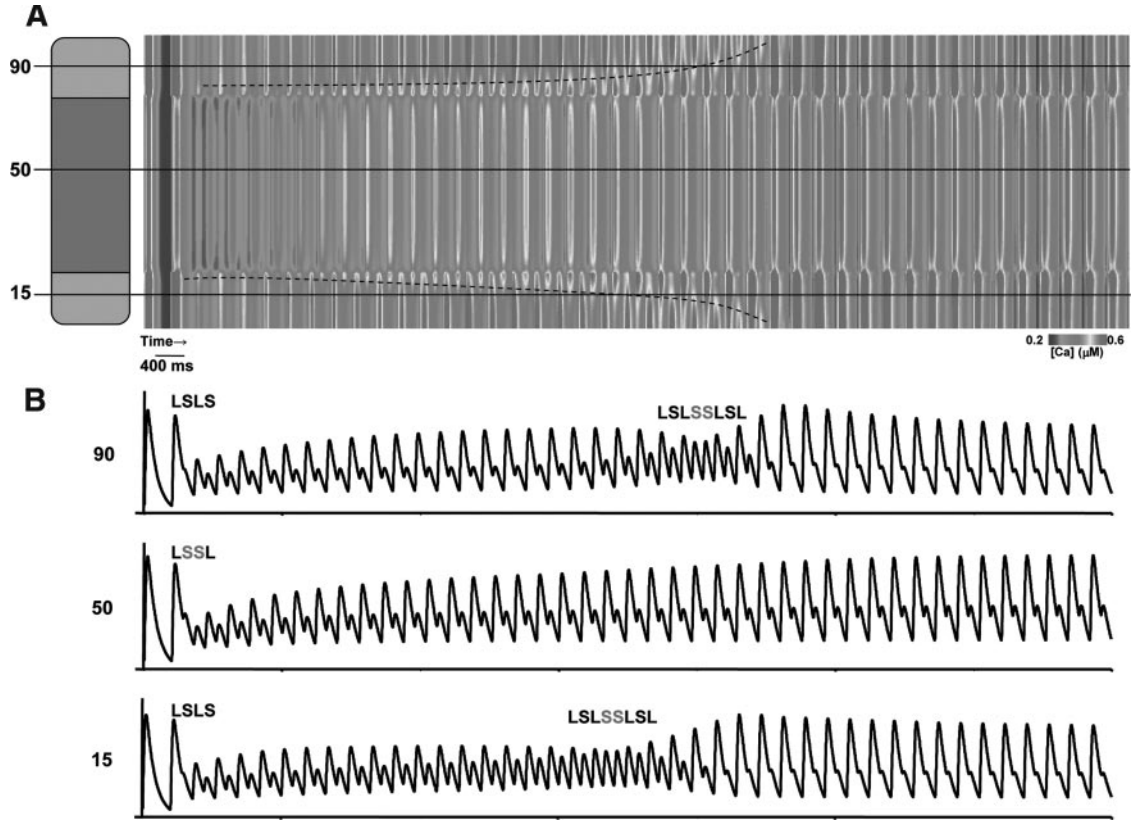

Figure 4. Simulations of CaT alternans in the absence of CL alternans. A, X-t plots of CaT vs time for 100 coupled sarcomeres during a decrease of pacing CL from 400 to 200 ms. Ca cycling is made heterogeneous by letting sarcomeres 20 to 80 (dark gray region) have different SR Ca release properties than sarcomeres 1 to 19 and 81 to 100 (light gray region). B, Plot of $[Ca]_i$ vs time for sarcomeres 15, 50, and 90.

that form at the heterogeneities drift and extinguish at the cell boundaries.

Evolution of Phase-Mismatched Alternans: Alternating CL

Our modeling studies showed that the spatiotemporal dynamics observed in Figure 1A can be reproduced simply by incorporating heterogeneity between sarcomeres. In contrast, we found that it is necessary to incorporate CL alternans in combination with heterogeneity between sarcomeres to reproduce the dynamic behavior seen in Figure 2A and 2B. To model heterogeneity, we let the release load slope vary across the cell so that $u=15$ sec^{-1} for sarcomeres 1 to 19 and 81 to 100 and $u=10$ sec^{-1} for sarcomeres 20 to 80. We paced the cell with an alternating CL defined as $CL(n)=CL+(-1)^n\Delta CL$, where $CL(n)$ is the CL on the nth beat, following a change in CL from 500 to 200 ms. In Figure 5A, we plot $[Ca]_i$ versus time across the cell, and in Figure 5B we plot $[Ca]_i$ versus time for sarcomeres 15, 50, and 90. In this case, we let ΔCL increase linearly from 0 to 9 ms over 50 beats. In Figure 5B, CaT alternans are phase-matched over the first 25 beats but gradually diminish in amplitude and then eventually reverse phase. However, sarcomere 50 reverses phase at time t_1, whereas sarcomeres 15 and 90 reverse phase at time t_2. On examining the node positions in the line scan image in Figure 5A (white dashed lines), the nodes form at time t_1 at the boundaries separating the 2 regions of different release load slope. These nodes then gradually drift toward the cell boundaries and extinguish, leaving phase-matched alternans throughout the cell.

Discussion

Change in CL in Conjunction With Ca-Cycling Heterogeneity Leads to Phase-Mismatched CaT Alternans

Our experimental studies revealed that when the CL is suddenly decreased, the beat-to-beat evolution of CaT alternans can differ substantially between sarcomeres. Therefore, as CaT alternans develop during rapid pacing, sarcomeres in different regions of the cell can become phase-mismatched. Subcellular alternans can develop within just the first 3 to 4 beats after the change in cycle length, which is reproduced by our mathematical model of coupled sarcomeres. The mechanism for this is simply that the phase of CaT alternans is chosen by the dynamical response of Ca cycling during the first few beats, and because Ca-cycling characteristics differ between sarcomeres, different sarcomeres are likely to develop CaT alternans that are phase-mismatched. Moreover, once CaT alternans develop, Ca diffusion between sarcomeres is not sufficient to resynchronize these phase-mismatched sarcomeres.

There have been few studies of the intrinsic heterogeneity in Ca release properties that could explain these observations. The use of confocal microscopy to study CaTs in cardiac

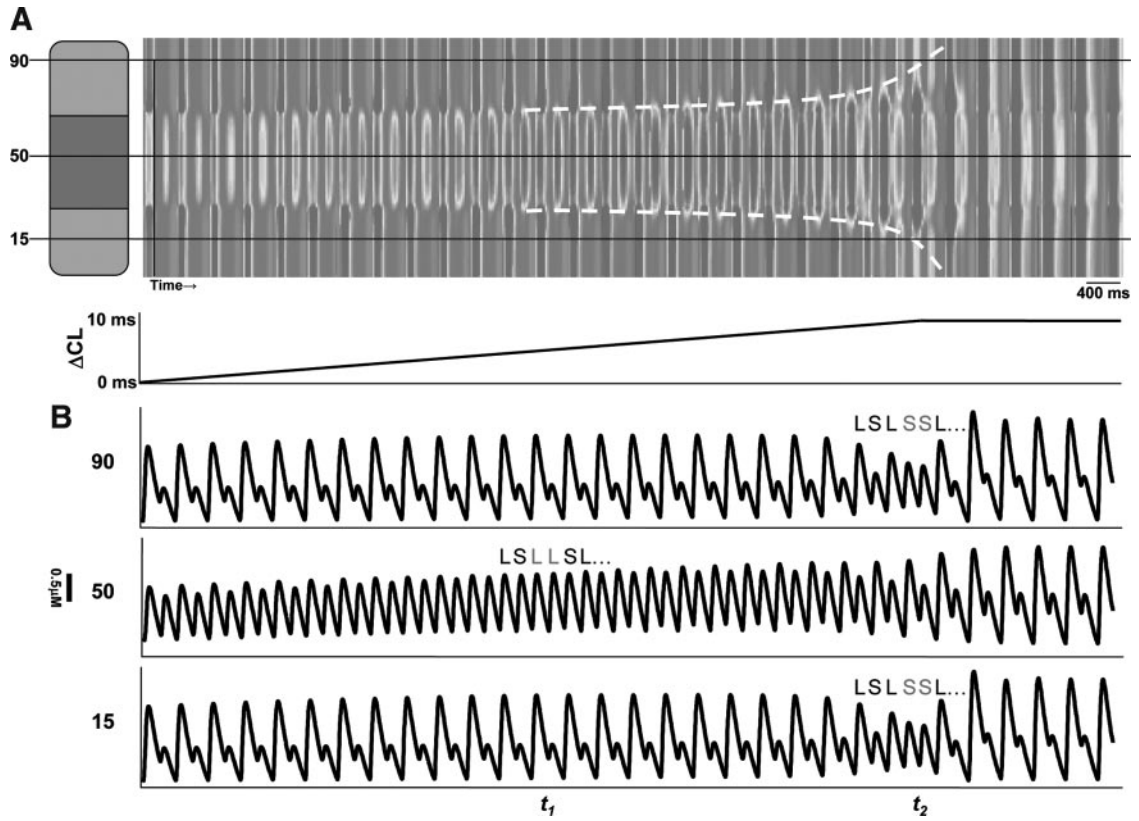

Figure 5. Simulations of CaT alternans in the presence of CL alternans. A, Heterogeneity was introduced by letting sarcomeres 20 to 80 have different Ca release characteristics from sarcomeres 1 to 19 and 81 to 100. The cell is paced at a CL of 500 ms and then switched to an alternating CL given by $CL(n)=CL+(-1)^n\Delta CL$, where CL=200 and ΔCL increases from 0 to 9 ms, as indicated in the bottom graph. Node location is shown in the white dashed line. B, Plot of $[Ca]_i$ vs time for sarcomeres 15, 50, and 90.

myocytes allowed the identification of substantial variation in release magnitude and timing along the cell length.[23] However, it was only recently that the heterogeneity in virtually all characteristics of intracellular Ca cycling was recognized in intact heart (Figure 1C and 1D).[3] This study shows that these characteristics have important influences on physiological behavior, especially during rapid pacing.

A key ingredient in the formation of phase-mismatched CaT alternans is the presence of variations of Ca-cycling properties across the cell. We modeled this effect in the numeric simulations by letting the SR Ca release properties vary across the cell. However, we found similar results when we varied LCC, NCX, or SERCA channel density (results not shown). The crucial requirement is simply that there are differences in the Ca-cycling response of different sarcomeres, which can arise because of a multitude of factors which influence Ca cycling. This is expected because Ca cycling is dependent on both Ca release from the SR and the Ca flux balance across the cell membrane, which is dependent on a wide variety of channels and pumps. Experimentally, it is also difficult to identify the specific protein(s) responsible for the observed heterogeneities but such spatial variations in RyR, SERCA, NCX, or LCC protein density are not unexpected. The novel finding in this article is that these differences can induce phase-mismatched Ca release patterns.

Node Movement Is Dictated by the Membrane Potential

Our experiments have shown that the spatial distribution of CaT alternans within a cell is time-dependent. In particular, nodes that mark the boundaries between regions of the cell that are phase-mismatched can drift across the cell. In Figure 6A and 6B, we show 2 examples where nodes move across a cell. To uncover the underlying mechanism for this effect, we first note that because cardiac cells in tissue are electrically coupled, the voltage across the membrane of a given cell is the spatial average of all cells within the electrotonic space constant. Thus, to a good approximation, the cell in the field of view is essentially driven by a voltage clamp. Furthermore, we expect that the voltage time course driving a cell can itself exhibit APD alternans. This is expected because a close examination of the pseudo-ECG reveals repolarization alternans, which suggests that beat-to-beat alternations exist in the local AP. Also, because Ca release is coupled to voltage via membrane currents, CaT alternans will induce APD alternans.[8] Furthermore, there is increasing evidence that repolarization alternans recorded in single cells of intact tissue reflects T-wave alternans at the level of intact myocardium, so that cellular phenomena reflect electrical behavior in the heart.[24] Note that the magnitude of APD alternans is sensitive to the average over all cells within the electrotonic space constant, which need not average to 0. Investigating the effect of APD alternans on the spatiotemporal dynamics of CaT

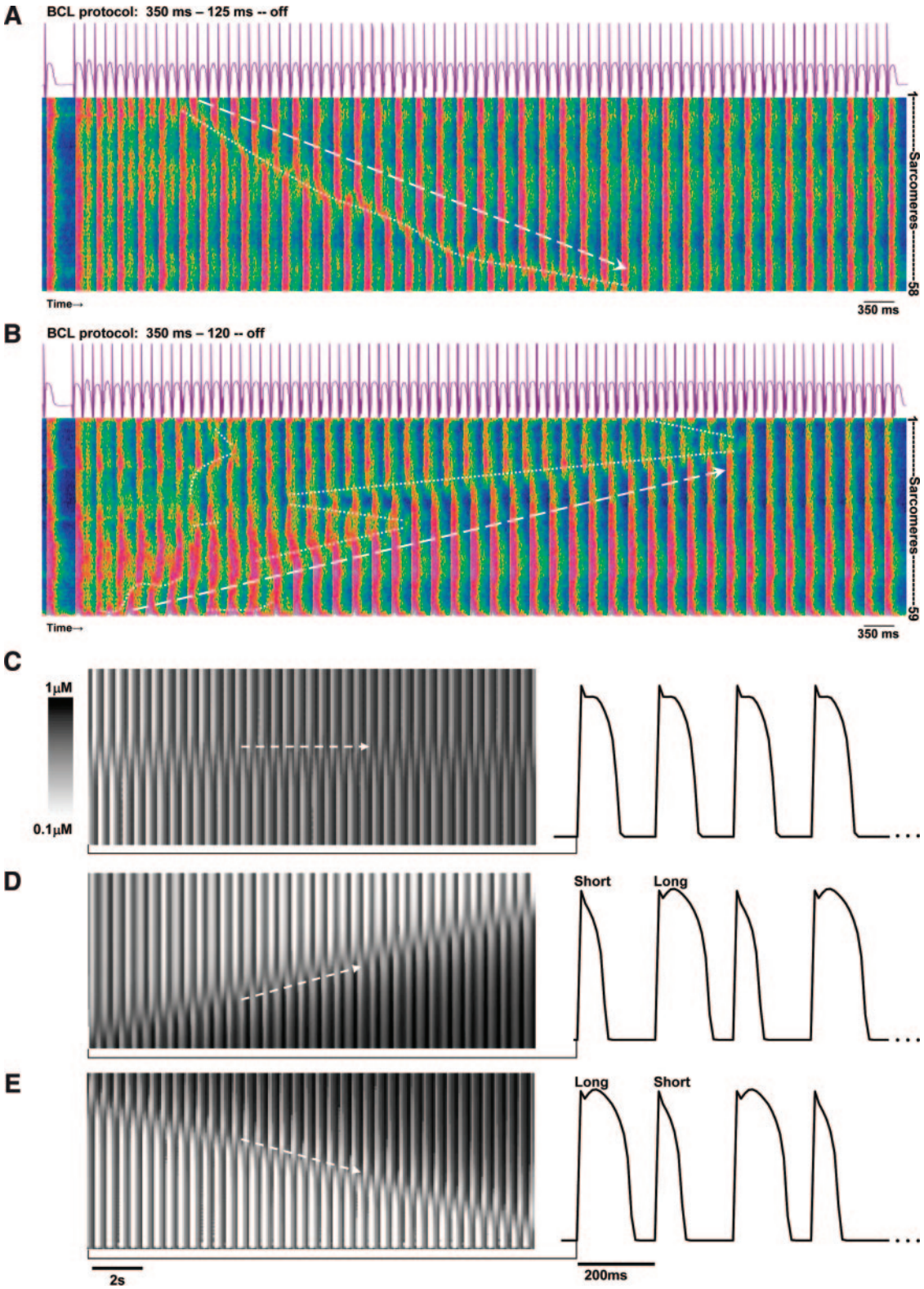

Figure 6. Simulations of CaT alternans nodes under AP clamp pacing. A, Line scan image acquired from a myocyte in which subcellular alternans developed at one end and traveled to the other end, where it was extinguished. B, Line scan image acquired from an adjacent myocyte to that in A (at faster rate) but with several nodes whose direction of travel is opposite to A. C through E, Simulation results of homogeneous cell with 100 sarcomeres paced by AP clamp. Phase-mismatched alternans are induced by choosing initial conditions so that sarcomeres 1 to 49 are phase-mismatched with those of sarcomeres 50 to 100. The time evolution of nodes is shown under the following conditions: periodic voltage clamp (C); a S-L-S-L voltage clamp (D); a L-S-L-S voltage clamp (E).

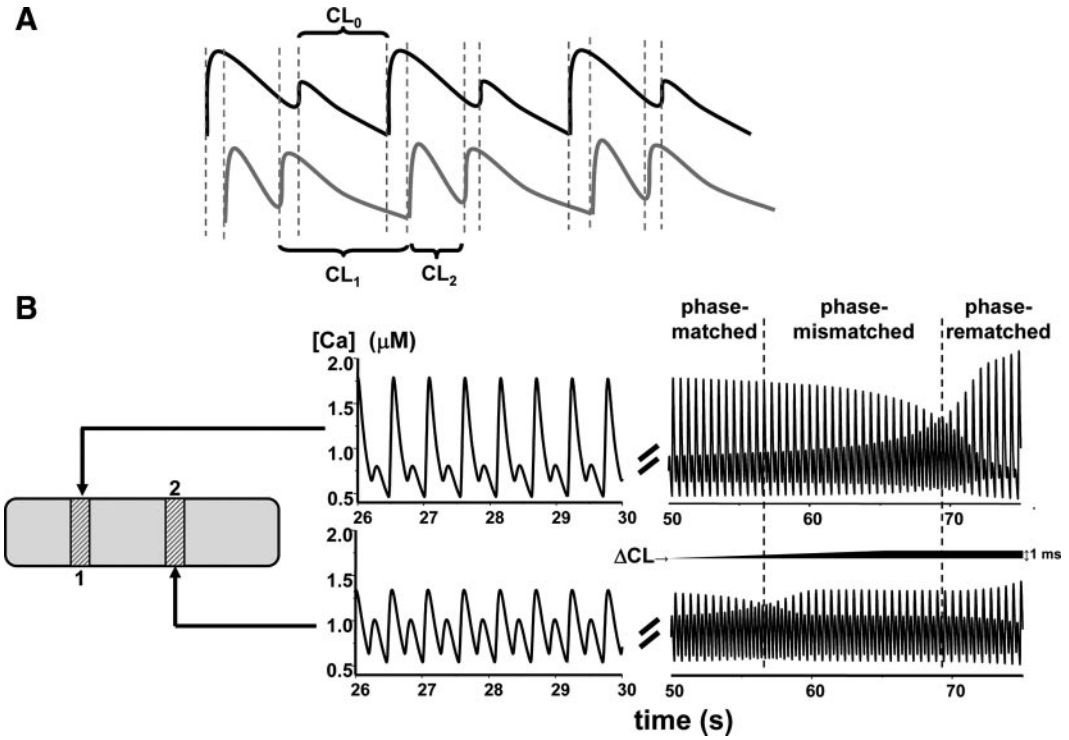

Figure 7. Simulations demonstrating proposed mechanism for phase reversal induced by CL alternans. A, Illustration of the effect of pacing a sarcomere with an alternating CL as shown. The long (short) CL is paired with the small (large) Ca transient. B, Mechanism for CL alternans-induced subcellular CaT alternans during constant rapid stimulus pacing: sarcomeres 1 and 2 are paced to steady state at a CL=250 ms but are not identical in that sarcomere 1 (u=12 sec^{-1}) exhibits a larger amplitude of alternans than sarcomere 2 (u=10 sec^{-1}). At time t=40 seconds, ΔCL is slowly increased so that sarcomere 2 reverses phase (left-most dashed line), and sarcomere 1 reverses phase more than 10 seconds later (right-most dashed line). Subcellular CaT alternans develops between the 2 dashed lines.

alternans reveals that the movement of nodes is dictated by the phase of APD alternans driving that cell. To support this claim, we simulated a cardiac cell that is paced by an alternating voltage clamp waveform. Within this cell, we form phase-mismatched alternans by simply choosing initial conditions so that half of the cell is phase-mismatched with the other half. As shown in Figure 6C, when the cell is paced with a periodic AP waveform, the CaT node does not move. However, if the AP wave form exhibits alternans with a given phase of L-S-L-S or S-L-S-L, then the node moves either up or down, respectively (Figure 6D and 6E). Once the node reaches the cell boundary, all sarcomeres in the cell are phase-matched, such that a large (small) CaT corresponds to a long (short) APD.

Our numeric simulations demonstrate that the presence of APD alternans leads to node movement. The mechanism for this effect is that when APD alternans of a given phase drive a sarcomere, that sarcomere will reverse its phase to match the phase of the APD alternans, such that CaT alternans will synchronize to the APD alternans. Thus, if the APD alternates in a L-S-L-S duration, then CaT alternans at the sarcomeric level will adjust to a L-S-L-S phase. This response is attributable to the fact that a large APD is followed by a short diastolic interval, reducing the recovery from inactivation of the LCC. Therefore, in the subsequent beat, there are fewer LCC openings, leading to decreased Ca release. APD alternans will then "force" sarcomere CaT alternans to synchronize their phase. If there is phase mismatch attributable to subcellular heterogeneities, then nodes will move so that the phase synchronized with the APD alternans driving the cell will gradually dominate. In contrast, in the absence of APD alternans and the AP is periodic from beat-to-beat, there is no mechanism to dictate which phase a particular sarcomere will obey, and the nodes remain fixed at the location at which they are formed. Dynamical changes in local Ca-cycling properties can only serve to enhance or diminish local CaT alternans amplitude but cannot impose a particular phase. Therefore, it is essential to invoke alternans in the AP waveform to explain node movement.

CL Alternans Are Necessary for Late Development of Phase-Mismatched CaT Alternans

Our experimental results also revealed that subcellular CaT alternans can exhibit a variety of distinct spatiotemporal dynamics. We found numerous instances where phase-matched alternans was established after many beats, after which multiple nodes formed spontaneously at the ends (and centers) of the cells and drifted toward the centers (and ends). Now the mechanism for node movement presented in the previous section could not explain these features because once APD alternans is synchronized with the CaT alternans throughout the cell, there is no mechanism for phase reversal and the cell should remain phase-matched. In these examples, however, we found a beat-to-beat CL alternans so that these cells were not paced at a truly constant CL. CL alternans is not unexpected because the conduction velocity of an elec-

trical wave in cardiac tissue is sensitive to the diastolic interval. Therefore, if the APD alternates from beat-to-beat, then so will the diastolic interval, and this will lead to an alternation of the conduction velocity in cardiac tissue. The result is that the time of arrival of a wavefront at the cell within the mapping field will typically alternate between beats. The mechanism for the transition from phase-matched to phase-mismatched and then back to phase-matched CaT alternans is attributable to a combination of CL alternans and the differences in Ca cycling between different sarcomeres. As illustrated in Figure 7A, let us first assume that a cell is paced at a constant cycle length CL_0 and that CaT alternans are present (indicated by the black line). In this case, the magnitude of alternans is determined simply by the relationship between SR Ca load and release. Now let us assume that this cell is then paced with a CL that alternates between a long (CL_1) and short (CL_2) duration. Here, the timing of the current stimulus is such that an early stimulus is delivered just before (after) the small (large) CaT. This choice of timing will serve to diminish the magnitude of alternans because the short CL favors a decrease in Ca release because that sarcomere will have less time to reload its SR. On the other hand, the long CL will lead to an increase in the small CaT because that sarcomere will have more time for reloading. Thus, the effect of an alternating CL on the Ca-cycling dynamics will be to diminish alternans and subsequently to reverse the phase of the alternans sequence as the amplitude of CL alternans is increased. For CL alternans to reverse the phase of CaT alternans, they must be out-of-phase in the sense that a long (short) CL must correspond to a small (large) Ca release. A close examination of the line scan images in Figure 3A and 3B is consistent with this prediction.

To explain the formation of subcellular CaT alternans, it is necessary to invoke the intrinsic differences between sarcomeres. In Figure 7B, we pace 2 sarcomeres with different Ca-cycling characteristics in which sarcomere 1 exhibits a larger degree of CaT alternans than sarcomere 2 at steady state. If we now pace these 2 sarcomeres with an alternating CL, then CaT alternans in both sarcomeres gradually diminish and reverse phase via the mechanism discussed above. However, the amplitude of alternans in sarcomere 1 decreases more slowly than that in sarcomere 2 and the phase-reversal points, as indicated by the vertical dashed lines, occur at different time points. Therefore, CaT alternans in both sarcomeres will be phase-mismatched during that time interval. Thus, the spatiotemporal dynamics observed in Figure 3A and 3B is caused by the interplay between CL alternans and the spatial variation of Ca-cycling characteristics.

This result highlights, for the first time, how dynamic factors, such as CaT and CL alternans, interact with heterogeneities at the sarcomere scale to form subcellular CaT alternans. These mechanisms could be of considerable clinical importance because subcellular alternans could promote the development of intracellular Ca gradients and resulting Ca waves, thus providing a mechanism for triggered activity and arrhythmias.[2,14]

Sources of Funding

Supported, in part, by The Everett-O'Connor Trust (A.H.K.). Computer simulations conducted by Yohannes Shiferaw were funded, in part, by American Heart Association Grant 0830298N.

Disclosures

None.

References

1. Bers DM. Cardiac excitation-contraction coupling. *Nature*. 2002;415:198–205.
2. Kockskamper J, Blatter LA. Subcellular Ca2+ alternans represents a novel mechanism for the generation of arrhythmogenic Ca2+ waves in cat atrial myocytes. *J Physiol*. 2002;545:65–79.
3. Aistrup GL, Kelly JE, Kapur S, Kowalczyk M, Sysman-Wolpin I, Kadish AH, Wasserstrom JA. Pacing-induced heterogeneities in intracellular Ca2+ signaling, cardiac alternans, and ventricular arrhythmias in intact rat heart. *Circ Res*. 2006;99:e65–73.
4. Qian YW, Clusin WT, Lin SF, Han J, Sung RJ. Spatial heterogeneity of calcium transient alternans during the early phase of myocardial ischemia in the blood-perfused rabbit heart. *Circulation*. 2001;104:2082–2087.
5. Hayashi H, Shiferaw Y, Sato D, Nihei M, Lin SF, Chen PS, Garfinkel A, Weiss JN, Qu Z. Dynamic origin of spatially discordant alternans in cardiac tissue. *Biophys J*. 2007;92:448–460.
6. Weiss JN, Karma A, Shiferaw Y, Chen PS, Garfinkel A, Qu Z. From pulsus to pulseless: the saga of cardiac alternans. *Circ Res*. 2006;98:1244–1253.
7. Qian YW, Sung RJ, Lin SF, Province R, Clusin WT. Spatial heterogeneity of action potential alternans during global ischemia in the rabbit heart. *Am J Physiol Heart Circ Physiol*. 2003;285:H2722–H2733.
8. Chudin E, Goldhaber J, Garfinkel A, Weiss J, Kogan B. Intracellular Ca(2+) dynamics and the stability of ventricular tachycardia. *Biophys J*. 1999;77:2930–2941.
9. Karma A. Electrical alternans and spiral wave breakup in cardiac tissue. *Chaos*. 1994;4:461–472.
10. Shiferaw Y, Sato D, Karma A. Coupled dynamics of voltage and calcium in paced cardiac cells. *Phys Rev E Stat Nonlin Soft Matter Phys*. 2005;71(2 pt 1):021903.
11. Diaz ME, O'Neill SC, Eisner DA. Sarcoplasmic reticulum calcium content fluctuation is the key to cardiac alternans. *Circ Res*. 2004;94:650–656.
12. Shiferaw Y, Watanabe MA, Garfinkel A, Weiss JN, Karma A. Model of intracellular calcium cycling in ventricular myocytes. *Biophys J*. 2003;85:3666–3686.
13. Diaz ME, Eisner DA, O'Neill SC. Depressed ryanodine receptor activity increases variability and duration of the systolic Ca2+ transient in rat ventricular myocytes. *Circ Res*. 2002;91:585–593.
14. Blatter LA, Kockskamper J, Sheehan KA, Zima AV, Huser J, Lipsius SL. Local calcium gradients during excitation-contraction coupling and alternans in atrial myocytes. *J Physiol*. 2003;546:19–31.
15. Wehrens XH, Lehnart SE, Marks AR. Intracellular calcium release and cardiac disease. *Annu Rev Physiol*. 2005;67:69–98.
16. Clusin WT. Calcium and cardiac arrhythmias: DADs, EADs, and alternans. *Crit Rev Clin Lab Sci*. 2003;40:337–375.
17. Wit AL, Rosen MR. Pathophysiologic mechanisms of cardiac arrhythmias. *Am Heart J*. 1983;106:798–811.
18. Shiferaw Y, Karma A. Turing instability mediated by voltage and calcium diffusion in paced cardiac cells. *Proc Natl Acad Sci U S A*. 2006;103:5670–5675.
19. Sato D, Shiferaw Y, Garfinkel A, Weiss JN, Qu Z, Karma A. Spatially discordant alternans in cardiac tissue: role of calcium cycling. *Circ Res*. 2006;99:520–527.
20. Echebarria B, Karma A. Instability and spatiotemporal dynamics of alternans in paced cardiac tissue. *Phys Rev Lett*. 2002;88:208101.
21. Watanabe MA, Fenton FH, Evans SJ, Hastings HM, Karma A. Mechanisms for discordant alternans. *J Cardiovasc Electrophysiol*. 2001;12:196–206.
22. Aistrup G, Shiferaw Y, Wasserstrom JA, Sharma R. Spatiotemporal dynamics of subcellular Ca2+ alternans. *Biophys J*. 2008;94:1536-Pos. Abstract.
23. Cannell MB, Cheng H, Lederer WJ. Spatial non-uniformities in [Ca2+]i during excitation-contraction coupling in cardiac myocytes. *Biophys J*. 1994;67:1942–1956.
24. Shimizu W, Antzelevitch C. Cellular and ionic basis for T-wave alternans under long-QT conditions. *Circulation*. 1999;99:1499–1507.

SUPPLEMENT MATERIAL

Detailed Methods

***Real-time confocal Ca fluorescence (CaT) acquisition*.** Whole rat heart preparation and recording of CaTs at sarcomeric-level resolution in ventricular myocytes of intact epicardium has been described in detail elsewhere [1]. Briefly, excised hearts from adult Sprague-Dawley rats were perfused retrogradely via the aorta on a Langendorff apparatus with CO_2-bicarbonate-buffered Tyrode's solution supplemented with 2% bovine serum albumin (pH 7.3-7.4). Hearts were placed in a perfusion\superfusion chamber situated on the stage of an LSM510 confocal inverted microscope (Zeiss) setup (**Online Figure I A**, left), and loaded via recirculation with the fluorescent Ca indicator, fluo-4AM (Invitrogen-Molecular Probes) at 10-20 μM for 20 min. Excess fluo-4 was washed out for 15-20 min, after which 50 μM cytochalasin-D was added in the recirculating perfusate to stop contractions and the temperature set at either 35°C or at room temperature (RT; 20-24°C). The pH of the external perfusate was monitored with a mini-pH electrode (IQ Scientific Instruments) place in the chamber and adjusted as necessary via increasing or decreasing the amount of CO_2 bubbled into the bicarbonate-Tyrode's perfusate. The heart was pressed gently against the glass bottom of the tissue chamber to provide a nominally flat optical surface from which to record confocal images. Atria were crushed to eliminate sinus rhythm allowing a typically AV nodal intrinsic rhythm. Bipolar electrical stimulation was delivered via platinum electrodes hooked into the ventricle apex, and two AgCl-Ag wires were place in the bath such that they were on opposing sides of the LV. Small regions 1-3 cell layers beneath the surface of the left ventricle epicardium of the intact rat heart were examined for well

defined myocytes (**Online Figure I A**, right). The scan line was placed along the longitudinal axis of a single myocyte (**Online Figure I B**, left), and X-t linescan images (the maximum X resolution of the Zeiss C-Apochromat 40x 1.2 NA objective used is ~0.2 μm at a the 517 nm emission maxima for fluo-4; the t resolution, or scanning speed, was 1.92 ms per linescan acquisition; confocal X-Y-Z optical slice volume for the corresponding linescan acquisitions is 1-2 μm^3) were recorded during pacing episodes consisting 2.5 s of alternans-free baseline pacing—one rate per episode, the CL of which typically ranged from 500-350 ms at 35°C, 700-500 ms at RT—followed by 10 s of alternans-inducing rapid pacing—one rate per episode, the CL of which typically ranged from CL=160-100 ms at 35°C, 300-180 ms at RT—followed by 2.5 s of no pacing (to assess F_0 as well as intrinsic an/or triggered activity), after which baseline pacing was resumed until the next recording episode was acquired (**Online Figure I B**, right). Psuedo ECGs (pECG…red tracing between linescan images in **Online Figure I B-C**) were also simultaneously recorded (pClamp 8, Axon Instruments—Molecular Devices) in sync with the linescan image recordings via TL trigger from the LSM computer (local V_m is not recorded in this technique, as presently available voltage-sensitive fluorescent dyes presently used—i.e., di-4-ANEPPS—give only ~4-10% change in fluorescence for every 100 mV change in V_m). For analysis, linescans were partitioned into serially adjacent 2 μm "sarcomeric" sections (**Online Figure I C)** from which corresponding sarcomeric CaTs were individually extracted (select sarcomeric CaT F vs. t profiles shown below image in **Online Figure I C**) and analyzed for cycle-to-cycle spatiotemporal characteristics—e.g.: peak amplitude (F/F_0); integral (F/F_0•ms); cycle-to-cycle alternans ratio; cycle-to-cycle percent recovery; duration at 50%, 80%

and 90% recovery—TD_{50}, TD_{80} and TD_{90} (ms); post-stimulus initiation, peak and TD_{90} latencies (ms); 10-90% peak amplitude rise-time; 90-10% peak amplitude decay-time (ms); max +*dF/dt* (F/F_0 /ms); max -*dF/dt* (F/F_0 /ms); halfwidth (ms).

Mathematical model. To model the subcellular spatial organization of CaTA alternans, we divide the cell into 100 sarcomeres as illustrated in **Online Figure I D**. Each sarcomere is modeled using a set of ordinary differential equations describing Ca cycling within that sarcomere. The essential elements of the local Ca cycling machinery, which are based on the model of Shiferaw *et al.* [2], are illustrated in detail **Online Figure I D**. Ca entry into the k^{th} sarcomere occurs via L-type Ca channels (I_{Ca}^k) which triggers a Ca-induced-Ca release flux (J_{rel}^k) from RyR channels in the SR membrane. Once intracellular Ca concentration rises, uptake (J_{up}^k) pumps on the SR membrane are activated and pump Ca back into the SR. The Ca that enters into the cell via I_{Ca}^k is extruded out of the cell via the electrogenic NaCa exchanger (NCX) current (I_{NaCa}^k). The coupling between sarcomeres is modeled by introducing a diffusive flux between adjacent sarcomeres [3]. To model the membrane voltage [4], we assume that V_m is dictated by the average of the ionic currents over the whole cell. The membrane ionic currents, which govern the dynamics of V_m across the membrane surrounding a single sarcomere, are shown schematically in **Online Figure I D**. The ionic currents are formulated using a canine ventricular cell model [5]. The spatially uniform V_m across the cell membrane satisfies the standard equation of charge-conservation

$$\frac{dV}{dt} = -\frac{1}{C_m}\left(I_{Na} + I_K + I_{stim} + \sum_{k=1}^{N}\left[I_{Ca}^k + I_{NaCa}^k\right]\right) \quad (1)$$

where C_m is the cell membrane capacitance and N is the number of sarcomere units. The current I_{stim} is a small stimulus current injected into the cell which triggers the action potential.

In this study we investigated the effect of heterogeneity on the spatial distribution of subcellular CaTA alternans. To do this we endow each sarcomere with different Ca cycling characteristics. For simplicity, we focus on spatial variations of SR Ca release properties, since this is the variable which has the most direct effect on Ca cycling characteristics. To modulate Ca release we allow each sarcomere, or groups of sarcomeres, to have specific Ca release properties by simply controlling the slope, defined as the variable u, of the SR Ca release vs. SR Ca load relationship [2]. Therefore, the release-load slope depends on the sarcomere index k. This quantity gives a measure of the sensitivity of SR Ca release on SR Ca load, and is a lumped variable which includes the combined effect of RyR channel density, dyadic junction spacing, and RyR Ca sensitivity on both the cytosolic and luminal side.

1. Aistrup GL, Kelly JE, Kapur S, Kowalczyk M, Sysman-Wolpin I, Kadish AH, Wasserstrom JA. Pacing-induced heterogeneities in intracellular Ca2+ signaling, cardiac alternans, and ventricular arrhythmias in intact rat heart. *Circ Res*. 2006;99:e65-73.
2. Shiferaw Y, Watanabe MA, Garfinkel A, Weiss JN, Karma A. Model of intracellular calcium cycling in ventricular myocytes. *Biophys J*. 2003;85:3666-86.
3. Shiferaw Y, Karma A. Turing instability mediated by voltage and calcium diffusion in paced cardiac cells. *Proc Natl Acad Sci U S A*. 2006;103:5670-5.
4. Sato D, Shiferaw Y, Garfinkel A, Weiss JN, Qu Z, Karma A. Spatially discordant alternans in cardiac tissue: role of calcium cycling. *Circ Res*. 2006;99:520-7.
5. Fox JJ, McHarg JL, Gilmour RF, Jr. Ionic mechanism of electrical alternans. *Am J Physiol Heart Circ Physiol*. 2002;282:H516-30.

Online Figure I: Illustration of experimental acquisition and analysis of sarcomeric Ca transients, and of the computational cell model of coupled sarcomeres. A) *Left-to-right*, photos of confocal microscopy/whole rat heart/Langendorff perfusion and bath chamber apparatus, close-up of perfusion chamber containing whole rat heart, whole rat heart attached to Langendorff perfusion showing where a site where (inverted) confocal images of intact left ventricular epicardium myocytes might be acquired, and a typical X-Y framescan image showing a ~235μm^2 region of intact epicardial myocytes (outlined with di-8-ANEPPS staining), showing cell selected for longitudinal line scanning. **B)** *Left,* X-Y image of the selected cell showing position of superimposed scan line in blue for the line scan image to the right. *Right,* Ca transients (green fluo-4 fluorescence) evoked by baseline pacing at CL=500 ms followed by a jump to rapid pacing at CL=150 ms CL. **C)** Partitioning of the linescan image into serially adjacent ~2 μm "sarcomeric" sections from which corresponding sarcomeric Ca transients were extracted for analysis (examples are from sarcomeres 2, 17, 34, 51, 68 and 88 shown below). Red tracing between X-t linescan images is the corresponding pECG. **D)** Illustration of cell model. The cell is divided into 50-100 compartments representing sarcomeres. Each sarcomere is labeled with an index *k*. Neighboring sarcomeres are coupled via diffusion of calcium across the myoplasm and the SR network (NSR).

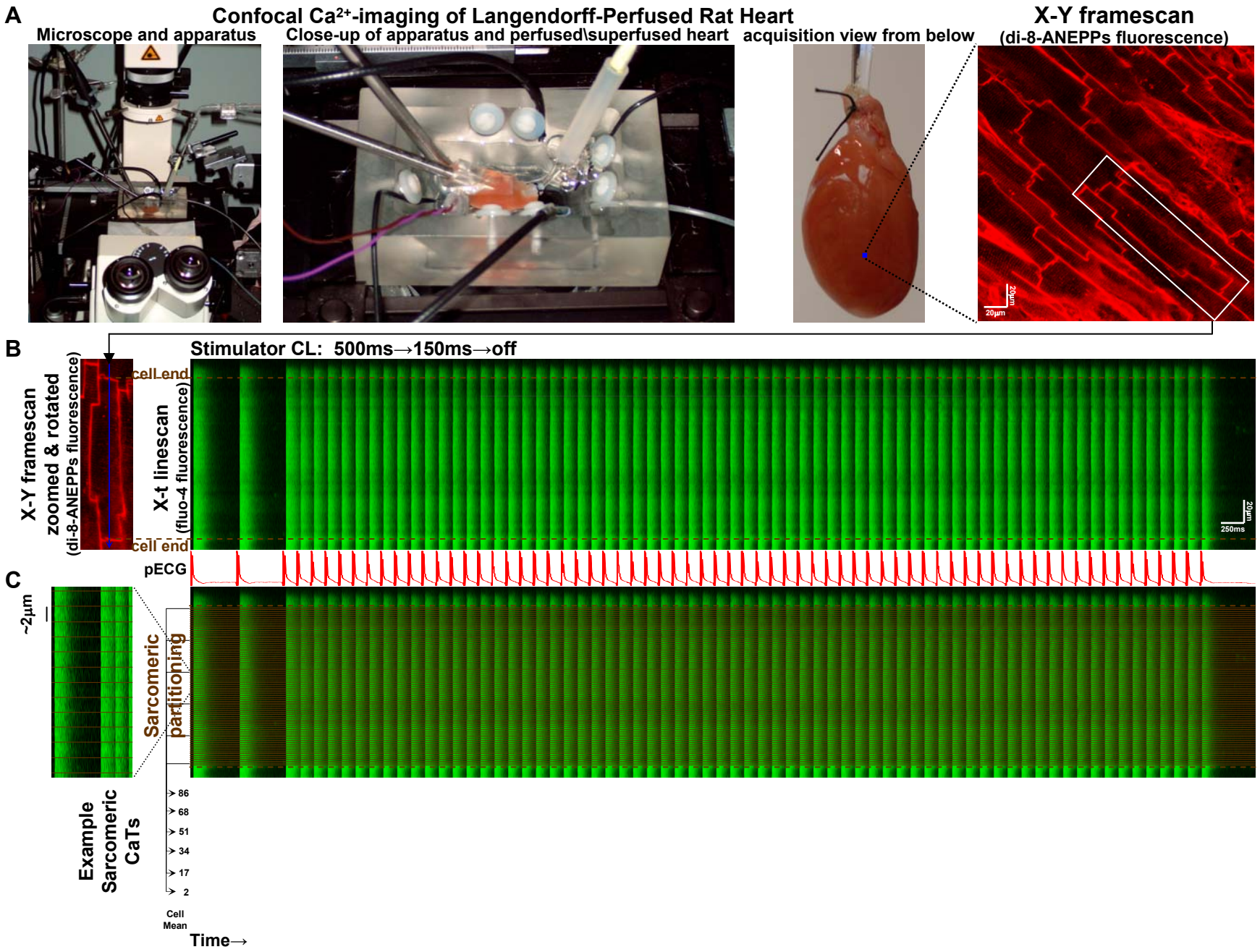

D